Onset of surface superconductivity

T. Giamarchi and M. T. Béal-Monod
Laboratoire de Physique des Solides, Université Paris–Sud 91405 Orsay, France

Oriol T. Valls*
Laboratoire de Physique des Solides, Université Paris–Sud, 91405 Orsay, France
and Center for the Science and Application of Superconductivity, School of Physics and Astronomy, University of Minnesota, Minneapolis, Minnesota 55455

(Received 8 November 1989)

We examine the onset of superconductivity in the surface region of a metal. Surface effects are particularly important in systems with a short bulk coherence length ξ_0. We show that, to the accuracy of the calculation, the surface transition temperature T_{cS} equals the bulk transition temperature T_{cB} if the electron-electron interaction is of the standard BCS form, i.e., a single attractive square well, extending up to some critical energy ω_0 much smaller than the Fermi energy ε_F. If one takes into account, in addition, the repulsive part of the interaction extending beyond ω_0 up to energies of order ε_F, then one may have $T_{cS} > T_{cB}$ in certain cases, although, due to restrictions imposed on the parameter values by various physical conditions, the relative increase of T_c is very small, typically 10^{-3}, at least in the weak coupling limit. However, we also find a considerable gap enhancement, of order 20%, near the surface which could be of interest for critical-current measurements. Therefore we suggest an experimental reexamination of systems with short ξ_0, i.e., superconducting degenerate semiconductors and the new high-T_c oxides in confined geometries where the surface-to-volume ratio is non-negligible.

I. INTRODUCTION

Boundary effects in standard superconductors have been extensively studied in the past.[1,2] In such systems, the coherence length ξ_0 is much larger than the interatomic distance (or the Fermi wavelength k_F^{-1}). Therefore the detailed modifications occurring in the properties of the system close the boundaries are of minor importance and can reasonably be neglected. The superconducting order parameter is thus well described by the Ginzubrg-Landau functional,[3] with suitable boundary conditions. Important results that have been obtained include the following. (i) The theory of H_{c3},[1,2] which shows that, in the presence of a magnetic field higher than H_{c2}, i.e., while the bulk of the sample is in the normal phase, a superconducting sheath nucleates at the surface. In that case however, the superconducting temperature T_c remains unchanged from its bulk value since, as explained above, the spatial variations of the order parameter near the surface are neglected. (ii) Dirty normal-superconductor sandwiches,[1] on the other hand, may exhibit transition temperatures significantly lower than those of the bulk. But in such case, it was emphasized[1] that the modifications very close to the interface are of minor importance compared to the diffusive behavior linked to the existence of a finite mean free path, while instead, in clean systems, the reflection and transmission aspects of the individual wave functions, on and through the interface, would play an important role. The particle-particle correlation function, in such dirty systems, was thus computed in the diffusive regime, via a method of images [under the form of the sum of two exponential functions of $(z+z')$ and $|z-z'|$, respectively, z and z' being measured perpendicularly to the surface]. It was later shown[4] that the correlation function actually contains extra terms, which are oscillatory functions of z and z', but are important only close to the surface, over a distance short compared to the conventional value of ξ_0, so that the hypotheses of Ref. 1 (amounting to the neglect of such terms) were justified. (iii) The study of quantum size effects in superconducting films,[5] and the variation of the transition temperature with thickness, again in the limit where ξ_0 is much larger than k_F^{-1}. (iv) The twinning-plane superconductivity[6] where the superconducting transition temperature is higher than that of either of the individual twin crystals. In such case too, a Ginzburg-Landau functional was used in the theory; the boundary condition contained an assumption which allowed one to satisfactorily explain that new phenomenon, i.e., the pairing attraction was supposed to be stronger near the twinning plane than deep in the bulk, possibly due to the combined effects of new soft two-dimensional phonon modes and a lattice density of atoms in the twinning-plane region lower than that in the bulk.

All of the preceding arguments (neglecting detailed structures over a few atomic distances from the surface, i.e., over distances much smaller than ξ_0) are indeed perfectly justified in conventional superconductors. However, in low-carrier-density materials such as oxide high-T_c superconductors (HTS),[7] where T_c is, at present, as high as 125 K,[8] the values of ξ_0 are considerably shorter (a few Fermi wavelengths), as one can see from BCS estimates [$\xi_0 = 0.180\hbar v_F/(k_B T_c)$, i.e., $k_F\xi_0 = 0.36 T_F/T_c$, where v_F and T_F are, respectively, the Fermi velocity and temperature]. Therefore those details of the boundary effects extending also over a few Fermi wavelengths from the sur-

face which are negligible in conventional superconductors with large ξ_0, may be expected to become important in the new high-T_c oxides with small ξ_0, and should be reexamined.

This is the purpose of the present paper. We will show that the full structure of the correlation function (oscillatory away from the surface as already noted in Ref. 4) becomes crucial. The bare particle-particle correlation function χ^0_{pp}, entering the BCS-type instability equation, is strongly modified compared to that of the bulk χ^{0B}_{pp}. We will investigate the influence of this geometrical effect on the gap function and also check whether the possibility exists of having a superconducting temperature in the surface region, T_{cS}, higher than the bulk one T_{cB}, in other words whether there exists a temperature range,

$$T_{cB} < T < T_{cS} , \tag{1.1}$$

for which, while the bulk of the sample is still normal, the surface region becomes superconducting. An objection could be raised here though, according to which a surface represents, for the electron gas of a clean system, a perturbation qualitatively similar to the presence of impurities in a dirty one, so that Anderson's theorem[9] should apply and thus T_c should not change compared to T_{cB}. However, as emphasized in particular in Ref. 10, Anderson's theorem applies only when the perturbation does not cause a long-range spatial variation of the order parameter, i.e.,[11] when the system is still homogeneous on the scale of the coherence length ξ_0. But, in the case we are considering, ξ_0 is of order of only a few k_F^{-1}, which is precisely the scale over which the order parameter is strongly modified near the surface, so that Anderson's theorem does not apply *stricto sensu* and thus a variation of T_c is allowed. We do indeed find that such an enhancement occurs in certain cases although the relative enhancement

$$\delta T_c/T_c \equiv (T_{cS}-T_{cB})/T_{cB}$$

that we have found is *very small,* at least in the region of parameter space that we have studied. To maximize $\delta T_c/T_c$ we should of course concentrate on cases with small ξ_0, i.e., large T_{cB} (which in itself is a big issue at present) or small T_F or both; obviously semimetals, doped semiconductors, etc., are candidates to be examined here, as well as high-T_c oxides. We doubt at present that geometrical effects alone can increase the surface T_c very much. The effects we discuss, however, could yield a more substantial increase when combined with that of Ref. 6 (i.e., a local increase in the strength of the pairing attraction $|V|$ near the boundary: $|V|+|\delta V|$). These two effects would complement each other since it is the product $V\chi^{0B}_{pp}$ that is involved in the BCS equation, which reads in the bulk,

$$1-V\chi^{0B}_{pp}=0 . \tag{1.2}$$

Both surface effects should be considered in small ξ_0 materials, when surface to volume atomic ratio is important, i.e., when there are many boundaries or if the system is of small size. The role in HTS of the second effect (changes in $|V|$) was recently pointed out.[12] We address here only the problem of the modifications in χ^0_{pp} near the surface.

In order to study possible surface superconductivity, we will use a simple jellium model to describe the free system in the normal state, with an infinite barrier at the surface. This will be done by analogy with another surface instability problem studied earlier,[13] the surface magnetism occurring in exchange-enhanced itinerant fermion systems which are paramagnetic in the bulk. We will show that, within our simple model, and even if the pairing interaction near the surface is identical to that in the bulk ($\delta V=0$), there are cases where a T_{cS} exists slightly larger than T_{cB}. We will also discuss how more realistic hypotheses are expected to act on such an increase of the critical temperature and what are the best candidates to optimize that increase. Perhaps more important, we will show that the order parameter amplitude is considerably enhanced at the surface of small ξ_0 superconductors even when the increase in the surface T_c is negligible.

The HTS are extremely complicated materials. The origin of the high-T_c values in these compounds is not yet clear. Going down in temperature from the normal phase [i.e., when $V\chi^{0B}_{pp}<1$ in (1.2)], various other factors may enter to increase the product $V\chi^{0B}_{pp}$ up to 1, so that T_c is increased too. One proposed factor[14] is a large increase in the density of states at the Fermi level $N(0)$ which enters into χ^{0B}_{pp}, due to two-dimensional Van Hove singularities possibly relevant in the layered structures of some of the HTS. In the present paper we restrict ourselves to a simplified study of a three-dimensional system with a parabolic band of fermions. We thus have the usual parameters characteristic of that case. Although the relative increase of T_c that we find is small, it could play a more general role in superconductors with small values of T_F/T_c or small ξ_0, which are in confined geometries or which contain multiple boundaries; in particular, the enhancement of the gap that we find near the surface is likely to play a role in the experimental values of the critical currents in the HTS films. Such effects have not yet, to our knowledge, been studied, except for the case of large ξ_0.[5]

II. THEORY

A. The Bethe-Salpeter equation of the surface superconducting instability

In this section, we examine a half-space itinerant fermion system, with a BCS type of mutual attraction $V<0$. The boundary breaks down translational invariance in the z direction, perpendicular to it. We suppose that it is planar and perfect, so we assume specular reflection on the surface. We wish to know how the presence of the surface possibly modifies the BCS instability criterion with V switched on as the temperature is decreased *from the normal phase.* Thus we examine at which temperature the system switches from the normal to the superconducting phase, that is, at which temperature the renormalized effective interaction in the particle-particle channel Γ_{pp} diverges. Γ_{pp} obeys a Bethe-Salpeter equation analogous to that for Γ^B_{pp}, the BCS bulk interaction

exhibited on Fig. 1, but with special surface boundary conditions. Our study will be made easier by using a close analogy with the case of Ref. 13 where a strong Hubbard-type contact repulsion $I>0$ acts between opposite spins, in a half-space itinerant paramagnetic fermion system. As in Ref. 13 the breakdown of translational invariance in the z direction perpendicular to the surface modifies the Bethe-Salpeter equation for the particle-particle correlation function. This quantity is given in the bulk by

$$\chi^B_{pp}=\chi^{0B}_{pp}+\chi^{0B}_{pp}V\chi^B_{pp} , \tag{2.1}$$

where the zero superscript refers to the noninteracting system and appropriate wave vector and frequency arguments are understood. In the presence of a surface an integration over the z direction remains and the Bethe-Salpeter equation takes an *integral* form which we write in the obvious shorthand form:

$$\chi_{pp}=\chi^0_{pp}+\int\chi^0_{pp}V\chi_{pp} . \tag{2.2}$$

Note that the *absence* of a specific bulk index indicates a surface quantity. As is the case of Ref. 13 for the particle-hole correlation function χ^0_{ph},[15] the particle-particle correlation function χ^0_{pp} is *not a separable kernel*, so that χ_{pp} cannot be calculated analytically and its possible divergence cannot yield a simple equation such as (1.2) in the bulk case, where it follows straightforwardly from (2.1). However, as in Ref. 13, numerical computations will show that χ_{pp} is considerably enhanced near the surface. The numerical computations, as well as a variational method similar to that in Ref. 13 will show that a superconducting surface instability occurs in certain cases for values of the dimensionless interaction for which the bulk is still in the normal phase.

Our calculations will be performed in terms of the renormalized vertex function Γ_{pp}. Γ_{pp} obeys an integral Bethe-Salpeter equation of the same form as (2.2). In the same shorthand notation we write

$$\Gamma_{pp}=V+\int\chi^0_{pp}V\Gamma_{pp} . \tag{2.3}$$

The numerical solution of (2.3) will yield the spatial dependence of the gap function.

B. The bare particle-particle correlation function near the surface, χ^0_{pp}

To perform our calculations we need first to compute χ^0_{pp} explicitly. The calculation of χ^0_{pp} is analogous to that of the particle-hole correlation function, χ^0_{ph}, done in Ref. 15. The algebra is cumbersome but straightforward and the main steps are given in Appendix A. The result is given by (A15). We find that, as in Ref. 15, χ^0_{pp} takes the form

$$\chi^0_{pp}(b,b')=D_{pp}(b)\delta_{b,b'}-A_{pp}(b,b') ,$$
$$b=q/(2k_F),\quad b'=q'/(2k_F) . \tag{2.4}$$

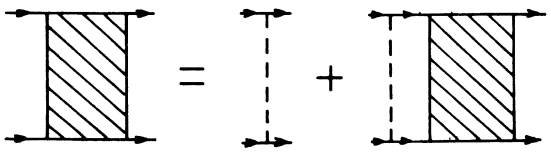

FIG. 1. The bulk Bethe-Salpeter equation for the renormalized interaction Γ^B_{pp}; the dotted line is the bare interaction V, the shaded square is Γ^B_{pp}; the straight lines are the electron lines.

D_{pp} and A_{pp} implicitly depend on the momentum parallel to the surface $\mathbf{K}_\parallel$, and the frequency ω [which was put equal to zero in (A15)], q and q' are the momenta in the z direction, and δ is the Kronecker symbol. Since the wave functions vanish at the surface, in real space χ^0_{pp} must vanish at $z=0$ for all z' and vice versa, since χ^0_{pp} is a symmetric function of z and z' (and of b and b' in Fourier space). This gives us a sum rule analogous to that in Ref. 15:

$$D_{pp}(b)=\int_0^{+\infty}A_{pp}(b,b')db' . \tag{2.5}$$

In the following, we restrict ourselves to the case $\mathbf{K}_\parallel=0$ (in addition to $\omega=0$) because we do not expect any significant structure in the parallel direction. Then, we use a suitable change of variables to transform the energy arguments of the Fermi functions in (A15) into the corresponding denominators:

$$\varepsilon_{1,2}=\varepsilon+\varepsilon_F(b\pm b')^2 ,$$
$$\varepsilon=\mathbf{k}_\parallel^2/2-\varepsilon_F \tag{2.6}$$

(in atomic units). We thus obtain, for the last two of the four terms of (A15):

$$-A_{pp}(b,b')=\frac{N(0)}{2}\int_{-\varepsilon_F}^{+\infty}\frac{\tanh\left[\frac{\varepsilon_1}{2T}\right]+\tanh\left[\frac{\varepsilon_2}{2T}\right]}{\varepsilon_1+\varepsilon_2}d\varepsilon , \tag{2.7}$$

where we exhibit the constant in front of the integral, and $N(0)$ is given (for one spin direction) by

$$N(0)=k_F/(2\pi^2) . \tag{2.8}$$

$D_{pp}(b)$ is more easily obtained through (2.5). $D_{pp}(0)$ is identical to χ^{0B}_{pp}, for zero total momentum and frequency. As in the bulk case, an upper cutoff on ε is needed in (2.7) to avoid the divergence in the integral when $\varepsilon\to\infty$. Such a cutoff is a physical quantity imposed by the definition of the interaction V in the Bethe-Salpeter equation (2.2) and we will discuss it shortly.

The two terms D_{pp} and A_{pp} appearing in χ^0_{pp} have the same meaning as the corresponding particle-hole quantities D_{ph} and A_{ph} in χ^0_{ph}, which were discussed in Ref. 13 (see, for instance, Fig. 1 in the second paper of Ref. 13). In real space, the D term corresponds to the sum of a bulklike diagram, plus its image with respect to the surface, which would thus depend, respectively, on $|z-z'|$ and $(z+z')$. These were the only terms retained in Ref. 1 in the problem of dirty normal-superconductor sandwiches recalled in the Introduction. In Ref. 1, however, these terms were studied in the diffusive regime and long wavelengths, yielding real-space functions exponen-

tially decreasing for increasing arguments, while in the present clean system, as in Refs. 13 and 15, the corresponding real-space functions oscillate with $|z-z'|$ and $(z+z')$. The A term corresponds instead to diagrams where one of the two particles scatters specularily from the surface between the end points $\mathbf{R}$ and $\mathbf{R}'$, while the other particle does not, so that the A contribution to $\chi^0_{pp}(z,z')$ depends on z and z' *separately*. This A term renders $\chi^0_{pp}(z,z')$ *nonseparable*, which, in turn, precludes the analytical solution of the Bethe-Salpeter equation (2.2). However it is precisely this A term that is responsible for the surface instability, as was emphasized in the magnetic case of Ref. 13. Indeed, suppressing the A term makes (2.2) straightforwardly soluble in Fourier space and yields the same type of instability as in the bulk. Therefore in order to check for a modification of the surface critical temperature with respect to the bulk, one must take into account the A term as we will do here. Moreover, due to the presence of the A term, momenta of order $2k_F$ and of order zero are equally important, which is another way of pointing out that in real space, the correlation functions cannot be reduced to exponentials (for which only vanishing momenta play a role). These functions oscillate with the arguments $(2k_Fz)$ and $(2k_Fz')$ and thus short wavelengths of order of the interparticle distance are crucial, as announced in the Introduction. Although the finite mean free path introduced in Ref. 1 for dirty sandwiches, would appear, *a priori*, sufficient to mimic the case of pure systems with short superconducting coherence lengths, the preceding arguments show that this is not quite so. A finite mean free path, accompanied by a diffusive regime, allows long wavelengths to prevail and the oscillations are lost. We therefore believe that the present formalism, preserving both long and short wavelengths, would be more appropriate to study clean systems that, for whatever reason, have short superconducting coherence lengths.

C. The interaction V and the cutoff in (2.7)

As we just mentioned, a natural cutoff arises from the Bethe-Salpeter equation in the bulk case as well as in the present one. In what follows, we will assume that the pairing attraction V is uniform all over the system, including the region close to the surface, i.e., we neglect the effect considered in Refs. 6 and 12 and we thus may *underestimate* the instability. We will later discuss the effect of possible changes in V as done in Refs. 6 and 12 and analogous to changes in I in the magnetic case of Ref. 16. For a uniform value of V, let us first recall the usual BCS arguments[17] for the bulk. We repeat here only some well-known features for the bulk to render the messier surface problem more transparent by comparison.

Consider Fig. 2. The two electrons have total incoming momentum $\mathbf{k}_1+\mathbf{k}'_1$ and frequency $\varepsilon_1+\varepsilon'_1$. The corresponding outgoing quantities are $\mathbf{k}_2+\mathbf{k}'_2$ and $\varepsilon_2+\varepsilon'_2$. From momentum and energy conservation, we have

$$\begin{aligned}&\mathbf{k}_1+\mathbf{k}'_1=\mathbf{k}_2+\mathbf{k}'_2=\mathbf{K}\ ,\\&\varepsilon_1+\varepsilon'_1=\varepsilon_2+\varepsilon'_2=\omega\ .\end{aligned}\tag{2.9}$$

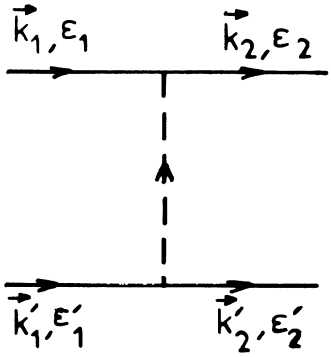

FIG. 2. The phonon mediated interaction between the two electrons in the BCS bulk problem.

Therefore the phonon-mediated BCS interaction has a momentum $\mathbf{Q}$ and frequency Ω such that:

$$\begin{aligned}&\mathbf{k}_2-\mathbf{k}_1=\mathbf{k}'_1-\mathbf{k}'_2=\mathbf{Q}\ ,\\&\varepsilon_2-\varepsilon_1=\varepsilon'_1-\varepsilon'_2=\Omega\ .\end{aligned}\tag{2.10}$$

In the standard jellium model for instance, the interaction $V(Q,\Omega)$ is given as a screened Coulomb potential in terms of the dielectric function $\varepsilon(Q,\Omega)$, which includes the phonon effects. These effects cause the interaction to be attractive when:

$$\Omega^2<\Omega_Q^2\ ,\tag{2.11}$$

where Ω_Q is a longitudinal phonon frequency.

The next step must be carefully analyzed as it will be most important in the surface case. One must introduce in all the BCS formulas a cutoff in energy, to avoid divergences in the integrals. Now, Ω in (2.10) is, strictly speaking, a *frequency difference*. However, one usually considers that on the energy shell one has

$$\Omega=\varepsilon(k_2)-\varepsilon(k_1)\ ,\tag{2.12}$$

$$\Omega=\varepsilon(k'_1)-\varepsilon(k'_2)\ ,\tag{2.13}$$

where the $\varepsilon(k)$ are the kinetic energies of the electrons. In standard BCS, the total momentum $\mathbf{K}$ in (2.9) is zero so that the two formulas (2.12) and (2.13) are consistently identical, while they would be different if $\mathbf{K}$ were finite. This taken for granted, a *sufficient but not necessary* condition for (2.11) to be fulfilled is that

$$\begin{aligned}&-\Omega_Q<\varepsilon(k_2)<\Omega_Q\ ,\\&-\Omega_Q<\varepsilon(k_1)<\Omega_Q\ ,\end{aligned}\tag{2.14}$$

and then, Ω_Q is taken to be a typical boson frequency ω_0 (the Debye frequency in the phonon BCS case), and one is left with the BCS assumption that $V(Q,\Omega)$ is a negative constant within (2.14) and zero outside:

$$\begin{aligned}V(Q,\Omega)&=-|V|,\quad |\varepsilon(k)|\le\omega_0\\&=0,\quad \text{outside}\ ,\end{aligned}\tag{2.15}$$

as indicated on Fig. 3(a). One may also wish to separate V into its attractive and its repulsive parts with the as-

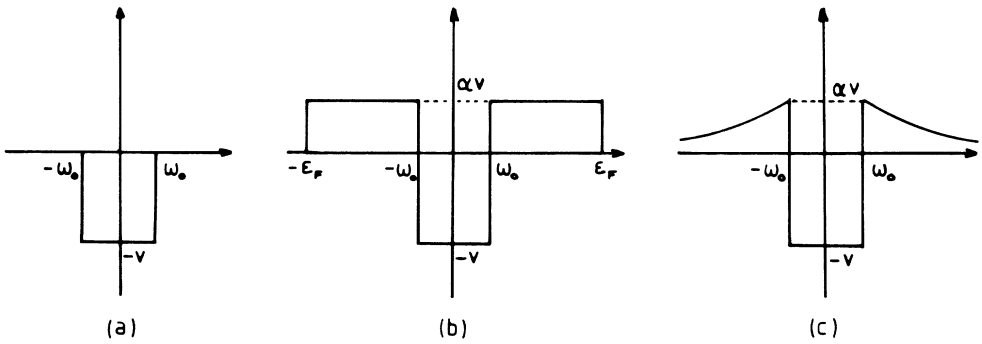

FIG. 3. The three models for the electron-electron interaction appearing in the text corresponding to formulas (2.22) and (2.23) and a model with analytic tails.

sumption that both of them are constant as indicated on Fig. 3(b) but with the repulsive part (representing, e.g., the Coulomb pseudopotential) extending beyond ω_0, up to the plasma energy, which is roughly of the order of ε_F. This is the Tolmachev two-square-well model extensively discussed and applied to superconducting semiconductors in Ref. 18. It is easy to check that, in this alternative, the main results of the BCS theory are not changed when compared to those obtained from the standard interaction of Fig. 3(a) except for multiplicative constants of order unity appearing in the formulas for T_c and for the gap function.

Returning to the standard model of Fig. 3(a) and in order to render the calculation of the bulk BCS equation tractable and eliminate all divergences, one usually sets the interaction equal to a constant v and introduces a cutoff in the energies of the incoming (or equivalently, the outgoing) electron lines. This leads to an effective vertex V which is *separable* and *symmetric*, through

$$\begin{aligned} &V=-vw_{k_1}w_{k_2}, \quad v>0 \\ &w_{k_1,k_2}=1, \quad |\varepsilon_{k_{1,2}}|<\omega_0 \\ &\qquad =0, \quad \text{elsewhere} , \end{aligned} \tag{2.16}$$

where k_1,k_2 are electronic momenta. In contrast, the two-square-well model of Fig. 3(b) is more difficult to write in such a form. In Ref. 18 it was shown that in this model one has to solve two coupled gap equations. One can avoid this complication by putting the cutoff asymmetrically, on only one line. This suffices to make all the integrals convergent and amounts to writing for V,

$$\begin{aligned} &V=-vw_{k_1}w_{k_2}, \quad v>0 \\ &w_{k_1}=1 , \\ &w_{k_2}=\begin{cases} 1, & |\varepsilon_{k_2}|<\omega_0 \\ -\alpha, & \omega_0<|\varepsilon_{k_2}|<\varepsilon_F \\ 0, & |\varepsilon_{k_2}|>\varepsilon_F . \end{cases} \end{aligned} \tag{2.17}$$

The symmetry of all the physical quantities involved in the calculation is properly preserved in the diagramatic perturbation calculation. In this procedure, one finds a bulk critical temperature somewhat lower than in the case when the attractive and repulsive parts are cut off at the same energy, while for the symmetric interaction it is higher.[18] However, this does not affect the issue of whether the surface transition temperature is the same as in the bulk. The preceding steps, for the bulk problem, must be then reexamined in the surface case.

D. The surface case

The Bethe-Salpeter equation for the vertex Γ_{pp} is illustrated on Fig. 4, where the contributions where one, both, or none of the two electrons scatter on the surface, are separately indicated. The first two contributions are obviously those of the bulk as given in Fig. 1. Let us consider in more detail in Fig. 5 one of the second-order contributions to Fig. 4. We have separated the momenta parallel to the surface (which will be treated as in the bulk, in particular we will later assume that $\mathbf{K}_{\parallel}=0$) from those perpendicular to the surface, which are the only ones affected by surface scattering, after which they change sign. Also because of the scattering, the sum of the two incoming perpendicular momenta, equal to $K_{1\perp}$ is not necessarily equal to that of the two outgoing momenta $K_{2\perp}$. However, at each individual vertex between the interaction line V and either one of the two electron lines, momentum is conserved; it follows that $k_{\alpha\perp}$ is fixed, given by

$$K_{1\perp}+K_{2\perp}=2k_{\alpha\perp} . \tag{2.18}$$

This fixed value of k_α illustrates that the D part of (2.4) in (A15) still involves a sum over k (the momentum perpendicular to the surface), but the A part does not.

Now let us consider the first interaction line of Fig. 5. It carries, equivalently to (2.10) in the bulk, a momentum $\mathbf{Q}$ and a frequency Ω such that:

$$\begin{aligned} &\mathbf{k}_{\alpha\parallel}-\mathbf{k}_{1\parallel}=\mathbf{Q}_{\parallel} , \\ &k_{\alpha\perp}-k_{1\perp}=Q_{\perp} , \\ &\varepsilon_\alpha-\varepsilon_1=\Omega . \end{aligned} \tag{2.19}$$

What we recalled for the bulk in connection with formu-

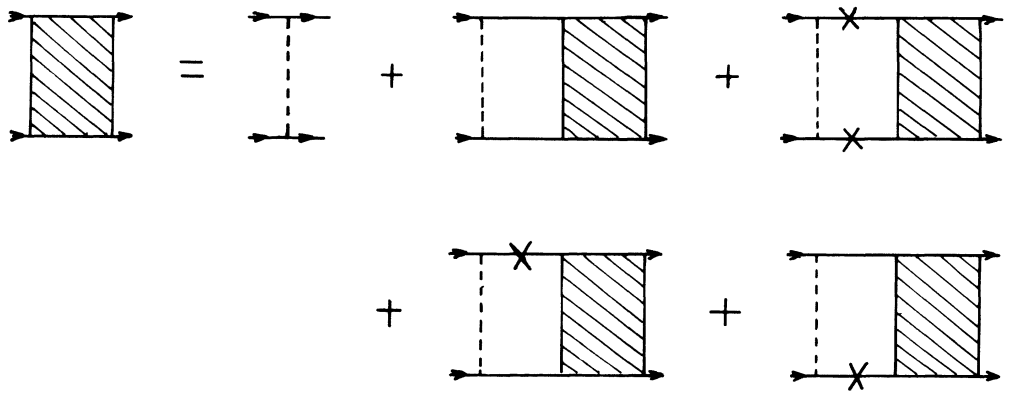

FIG. 4. The Bethe-Salpeter equation for Γ_{pp} in the surface case analogous to that in Fig. 1 for the bulk. The crosses correspond to scattering on the surface.

las (2.9)–(2.11) applies here too, but there are some differences. If we wished to write two formulas equivalent to (2.12) and (2.13), in order for them to be compatible we should restrict not only $\mathbf{K}_{\parallel}=0$, but also $K_{1\perp}=0$. However, as pointed out in Ref. 13 for the similar magnetic problem, a crucial role for surface instability is played by large values of $K_{1\perp}$, characteristic of the specific role of the surface. Therefore it is impermissible to use the approximate formulas (2.12) and (2.13) which would restrict $K_{1\perp}$ to be negligibly small, in which case only the bulk result would be recovered. If we recall that what is involved in (2.11) is, strictly speaking, the *frequency transfer,* identical to $\varepsilon_\alpha-\varepsilon_1$ here for *both* electron lines, the physics is the same regardless of the finite value $K_{1\perp}$ takes. We may then make an assumption of the form (2.14) (a sufficient but not necessary condition, as in the bulk) by writing

$$-\Omega_Q<\varepsilon_{k_1}<\Omega_Q\ ,\qquad -\Omega_Q<\varepsilon_{k_\alpha}<\Omega_Q\ , \tag{2.20}$$

thus choosing to restrict the kinetic energies of the upper electron line. The diagram analogous to that of Fig. 5 but with a cross on the lower electron line (contributing to the last diagram of Fig. 4) will symmetrize the entire procedure if we restrict there also the kinetic energies of the upper electron line. Inequalities of the form (2.20) will, according to (2.6), restrict either only $(b+b')$ or only $(b-b')$. Therefore there will always be cases where

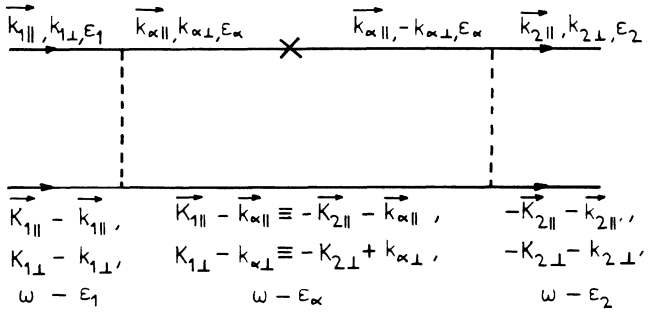

FIG. 5. The basic ingredient of Fig. 4 to second order in the interaction. Note that momenta conservation imposes that $K_{1\perp}+K_{2\perp}=2k_{\alpha\perp}$.

b, or b', or both may take large values, a condition that, in the magnetic case, is necessary to obtain a surface instability different from the bulk one. For the same reason (the important role of high ε_q values, i.e., high b and b' values) we will consider, in the following, not only the standard BCS structure for V of Fig. 3(a) but also that of Fig. 3(b). We could also consider different tail shapes. A model potential very close to that of Fig. 3(b) is shown in Fig. 3(c) where repulsive tails decreasing as the inverse energy replace the repulsive square well of Fig. 3(b). We checked that the potentials in Fig. 3(b) and 3(c) give qualitatively the same results and will present only work done with the former. These potentials allow, in the surface case, the influence of the higher values of b and b' to be felt [which the model of Fig. 3(a) does not] and they are therefore more likely to allow for a surface instability different from that in the bulk to take place. Furthermore, in Fig. 3, ω_0 may in all cases be identified either with Ω_D if the attraction is of phonon origin, or more generally, any other characteristic energy if the source of the attraction is nonphononic, provided only that $\omega_0\ll\varepsilon_F$.

We then will perform our calculations with

$$V=-vw_{k_1}w_{k_2},\quad v>0 \tag{2.21}$$

with the w chosen to correspond to Fig. 3:

model (a)

$$w_{k_1,k_2}=\begin{cases}1, & |\varepsilon_{k_1,k_2}|<\omega_0\\ 0, & \text{otherwise}\ ,\end{cases} \tag{2.22}$$

model (b)

$$w_{k_1}=1\ ,\qquad w_{k_2}=\begin{cases}1, & |\varepsilon_{k_2}|<\omega_0\\ -\alpha, & \omega_0<|\varepsilon_{k_2}|<\varepsilon_F,\quad 0<\alpha<1\\ 0, & |\varepsilon_{k_2}|>\varepsilon_F\ .\end{cases} \tag{2.23}$$

Similar expressions could be written for the potential in Fig. 3(c). The various cutoffs will then be reflected in the calculation of (2.7) as follows:

$$-A_{pp}(b,b')=\frac{N(0)}{4}\int_{-\varepsilon_F}^{+\infty}\frac{\{\tanh[\varepsilon_1/(2T)]+\tanh[\varepsilon_2/(2T)]\}}{\varepsilon_1+\varepsilon_2}[w(\varepsilon_1)+w(\varepsilon_2)]d\varepsilon \tag{2.24}$$

Note the already mentioned asymmetrical character of model (b). The calculation is symmetrized as indicated below (2.20). Each of the $w(\varepsilon_1)$ or $w(\varepsilon_2)$ is the product of two w_k's in (2.24), one of them being identical to unity according to (2.23).

III. RESULTS

A. Analytical considerations

We can now compute χ^0_{pp} [needed for Γ_{pp} in (2.3)] through (2.4) with (2.5) in which the physical cutoffs are imposed by (2.22) and (2.23). The superconducting instability will obviously arise as a solution of the homogeneous equation corresponding to (2.3), which we write in real space as

$$\Gamma_{pp}(z,z')=V\int\chi^0_{pp}(z,z'')\Gamma_{pp}(z'',z')dz' . \tag{3.1}$$

We focus on the integral over z' of Γ_{pp} which has the structure of the Gor'kov gap equation[3]

$$\Delta(z)=\int\Gamma_{pp}(z,z')dz' \tag{3.2}$$

with $\Gamma_{pp}(z,z')$ given now by (3.1). We thus get

$$\Delta(Z)=\bar{V}\int\overline{\chi^0_{pp}}(Z,Z')\Delta(Z')dZ' , \tag{3.3}$$

where the above-discussed cutoffs are understood and normalized quantities are defined as

$$\begin{aligned}&\bar{V}\equiv V\chi^{0B}_{pp} ,\\ &\overline{\chi^0_{pp}}(Z,Z')\equiv\chi^0_{pp}(Z,Z')/\chi^{0B}_{pp} ,\\ &Z\equiv 2k_F z,\quad Z'\equiv 2k_F z' .\end{aligned} \tag{3.4}$$

The superconducting instability equation (3.3) is the analog of the instability in the magnetization studied in Ref. 13.

At a given temperature $T=T_{cS}$ a surface instability occurs, from (3.3), at a value of V, $V=V_S$. At the same temperature, the bulk would be superconducting for a value $V_B=1/D(T_{cS},0)$, where we define $D(T_c,b)$ to be the expression of $D(b)$ at the temperature T_c. On the other hand, if we work with a fixed value of $V=V_S$, the bulk would be superconducting at a temperature T_{cB} given by $1=V_S D(T_{cB},0)$. Therefore we have

$$\bar{V}_S/\bar{V}_B=D(T_{cS},0)/D(T_{cB},0) , \tag{3.5}$$

which we find in some cases to be smaller than unity. One can show that the leading contributions to $\bar{V}_B$ and $\bar{V}_S$ may be written in the BCS form:[19]

$$\bar{V}_B=|V|N(0)\ln\left[\frac{4e^{\gamma}}{\pi}\frac{\omega_0}{2T_{cB}}\right] , \tag{3.6}$$

$$\bar{V}_S=|V|N(0)\ln\left[\frac{4e^{\gamma}}{\pi}\frac{\omega_0}{2T_{cS}}\right] , \tag{3.7}$$

where $e^{\gamma}\simeq 1.781$. This implies $T_{cS}>T_{cB}$ when $\bar{V}_S<(\bar{V}_B=1)$. As will be shown below $(T_{cS}-T_{cB})\ll T_{cB}$, and thus one can relate, in a first approximation, the variation of the coupling constant $\bar{V}$ to the variation of T_c by

$$\frac{\bar{V}_S-\bar{V}_B}{\bar{V}_S}=(T_{cS}-T_{cB})\frac{D'(T_{cB})}{D(T_{cB})} . \tag{3.8}$$

In Fourier space (3.3) reads

$$\Delta(b)=\bar{V}\int\overline{\chi^0_{pp}}(b,b')\Delta(b')db' , \tag{3.9}$$

which we rewrite as in Ref. 13 in Dirac notation

$$|\Delta\rangle=\bar{V}\overline{\chi^0_{pp}}|\Delta\rangle . \tag{3.10}$$

Thus we get

$$(1-\overline{\chi^0_{pp}})|\Delta\rangle=\bar{E}|\Delta\rangle \tag{3.11}$$

with

$$\bar{E}=1-1/\bar{V} \tag{3.12}$$

and we must look for the lowest eigenvalue $\bar{E}_S$ of (3.11). This can be done numerically. One can also use the approximate variational method of Ref. 13. If Δ_{tr} is a trial wave function, we will thus have the variational inequality

$$\bar{E}_S\le\frac{\langle\Delta_{tr}|1-\overline{\chi^0_{pp}}|\Delta_{tr}\rangle}{\langle\Delta_{tr}|\Delta_{tr}\rangle}\equiv F . \tag{3.13}$$

If we prove that $F<0$, then $\bar{E}_S<0$, which means from (3.12), $\bar{V}_S<1$, i.e., $\bar{V}_S<(\bar{V}_B=1)$. Therefore surface superconductivity then arises for a value of $\bar{V}$ for which the bulk is still in the normal state, i.e., at $T_{cS}>T_{cB}$.

We take a trial function of the same form as that in Ref. 13

$$\overline{\Delta_{tr}}(b)=\Delta_{tr}(b)/\chi^{0B}_{pp}=\frac{2\lambda}{\pi(\lambda^2+b^2)}-\theta(1-b) \tag{3.14}$$

with λ the variational parameter. In real space, as in Ref. 13

$$\overline{\Delta_{tr}}(Z)=\Delta_{tr}(Z)/\chi^{0B}_{pp}=e^{-\lambda Z}-\sin(Z)/Z . \tag{3.15}$$

When $\lambda\to 0$, $\overline{\Delta_{tr}}(Z)$ is very close to the natural quantity $N(Z)$ obtained from (3.2) with $\Gamma_{pp}(Z,Z')$ reduced to $\chi^0_{pp}(Z,Z')$ in the absence of interactions, as was the case for $m^0(Z)$ in Ref. 13. $N(Z)$ measures, as pointed out in Ref. 1, the spatial variations of the local density of states, near the surface. The algebra is then the same as that in Ref. 13 where it was shown that the denominator in (3.13) is proportional to λ^{-1}, when $\lambda\to 0$. In that limit the numerator may be evaluated to zeroth order in λ, which involves only $\overline{\Delta_{tr}}(b)\simeq\delta(b)-\theta(1-b)$ and then,

$$G \equiv \langle \overline{\Delta_{tr}} | 1 - \overline{\chi^0_{pp}} | \overline{\Delta_{tr}} \rangle$$
$$= \int [1 - \overline{D_{pp}}(b)][\overline{\Delta_{tr}}(b)]^2 db$$
$$+ \int\int \overline{A_{pp}}(b,b')\overline{\Delta_{tr}}(b)\overline{\Delta_{tr}}(b')\, db\, db' . \quad (3.16)$$

On physical grounds, $\overline{D_{pp}}(b) = D_{pp}(b)/D_{pp}(0)$ is even in b, thus $\overline{D_{pp}}(b) \sim 1 + O(b^2)$ when $b \to 0$. Therefore (3.16) reduces to

$$G = P_1 - P_2 \quad (3.17)$$

with

$$P_1 = 1 + \overline{A_{pp}}(0,0) - 2\int_0^1 \overline{A_{pp}}(b,0) db ,$$
$$P_2 = \int_0^1 db \int_1^\infty \overline{A_{pp}}(b,b') db' , \quad (3.18)$$

where $\overline{A_{pp}}(b,b') = A_{pp}(b,b')/D_{pp}(0)$. If the coefficient α of the repulsive part of the potential is zero, then the integrand in (2.24) is positive definite, $A_{pp}(b,b')$ and $D_{pp}(0)$ are negative, so that $\overline{A_{pp}}(b,b')$ and P_2 are positive. A surface instability ($F < 0$ or $G < 0$) will then necessarily occur when $P_1 \leq 0$. In the magnetic problem,[13] $P_1 = 0$, but this is not the case here, and we have to compute P_1 for the various models (2.21) and (2.23). When $\alpha > 0$, the sign of P_2 is no longer obvious. However, examination of the integrals involved leads one to expect that $P_2 \ll P_1$. In most cases the surface instability would thus depend only on the sign of P_1 even in the presence of repulsive interactions. This has been checked for all the models studied. Some values of P_1 and P_2 obtained by numerical integration are presented in Table I. In Appendix B we present the calculation of P_1 in detail for the two models (a) and (b). We find that, as in the magnetic case, the role of the high-energy values allowed by the repulsive tails of V in model (b) and in other models with repulsive tails that we have checked, as indicated at the end of the preceding section, is crucial for a surface instability to take place. The variational method proves that a surface instability can occur if the inequality (B18) for model (b) can be fulfilled, provided that P_2 is not too negative, which proved to be the case for all models studied. For model (a) the variational method is not conclusive in its analytical form and one can only use the numerical work.

TABLE I. Values of P_1 and P_2 obtained from a numerical integration for model (b). For all the values considered here $|P_1| \gg |P_2|$ and $P_1 - P_2 < 0$. The variational method of Sec. III A proves, therefore, the existence of a surface instability.

ε_F	ω_0	T	α	P_1	P_2
1 000	100	50	0.4	−0.3354	-0.60×10^{-1}
1 000	300	50	0.6	−10.91	-0.32×10^{-3}
1 000	300	50	0.8	−5.326	-0.62×10^{-3}
10 000	300	5	0.6	−7.311	−0.123
10 000	300	5	0.8	−3.7018	−0.167
10 000	300	50	0.5	−0.8309	−0.101

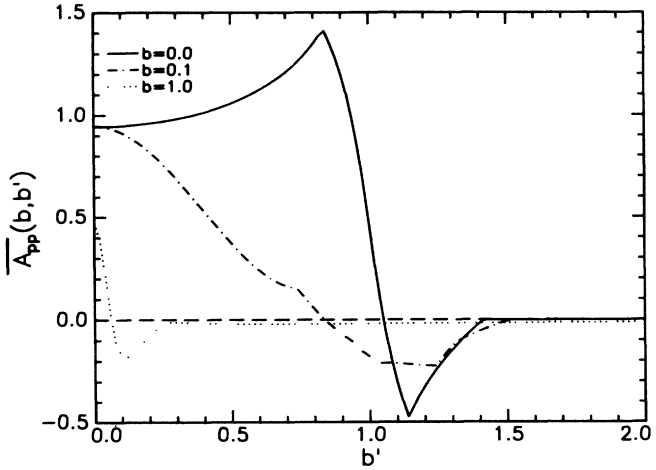

FIG. 6. $\overline{A_{pp}}(b,b')$ at $\varepsilon_F = 1000$, $\omega_0 = 300$, $T = 50$, and $\alpha = 0.8$ for several values of b as a function of b'.

B. The numerical results

For general values of the parameters it is impossible to solve (3.3) analytically but a numerical solution is always straightforward. We perform first a numerical integration to determine $A(b,b')$. An example of the results obtained is given on Fig. 6. Using the sum rule (2.5) it is possible to obtain $D(b)$ by an additional numerical integration, and the results are indicated in Fig. 7.

The gap equation in Fourier space (3.9) can be rewritten

$$\sigma\Delta(b) = \int \overline{\chi^0_{pp}}(b,b')\Delta(b')db' \quad (3.19)$$

with $\sigma \equiv 1/\overline{V}$. The problem is, as described previously, to find the largest eigenvalue and the corresponding eigenvector of the integral equation (3.19). For this purpose, the integral equation is reduced to an algebraic eigenvalue equation by replacing the integral by a sum. The largest eigenvalue of the matrix obtained is then

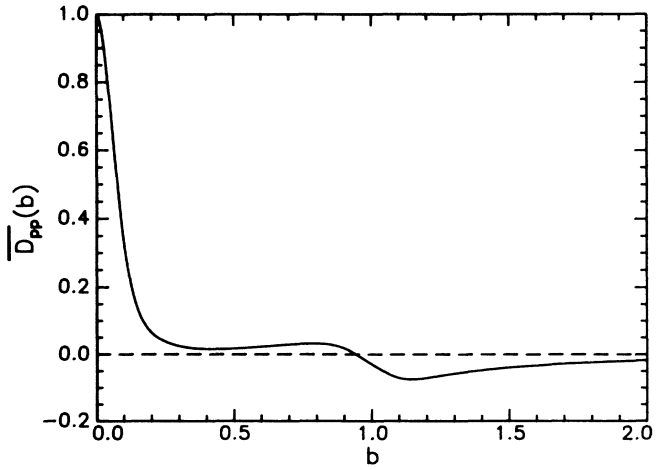

FIG. 7. $\overline{D_{pp}}(b)$ at $\varepsilon_F = 1000$, $\omega_0 = 300$, $T = 50$, and $\alpha = 0.8$ as a function of b. Notice that the maximum of $\overline{D_{pp}}(b)$ is always at $b = 0$, as expected physically since $\overline{D_{pp}}(b) = \chi^{0B}_{pp}$.

TABLE II. Some quantities calculated for model (b). Model (a) ($\alpha=0$) for the same values of the parameters, gives, up to the numerical accuracy, $\delta\bar{V}=0$ and thus $\delta T_c=0$. [Note that in weak coupling one is in principle limited to $-D_{\rm pp}(0)>1$.]

ε_F	ω_0	T	α	$(\bar{V}_B-\bar{V}_S)/\bar{V}_B$	$(T_{cS}-T_{cB})/T_{cB}$	$-D_{\rm pp}(0)$
1000	100	50	0.4	0.31×10^{-1}	0.26×10^{-2}	0.056
1000	300	50	0.6	0.25×10^{-3}	0.31×10^{-3}	1.23
1000	300	50	0.8	0.71×10^{-3}	0.72×10^{-3}	1.01
10000	300	5	0.6	0.12×10^{-4}	0.26×10^{-4}	2.16
10000	300	5	0.8	0.24×10^{-4}	0.35×10^{-4}	1.48
10000	300	50	0.5	0.7×10^{-4}	0.14×10^{-4}	0.20

computed, in order to get the smallest $\bar{V}$ for which a surface instability occurs. The discretization of the integral is the main source of numerical uncertainty. The discretization is performed for typically 200, 400, and 800 points and an extrapolation for an infinite number of points is performed in order to increase the precision of the results. Our results are accurate to five significant figures.

The parameters in the problem are the characteristic frequency ω_0, ε_F, and T. Only two of the ratios among these three quantities are independent parameters, however. Therefore we do not specify units for these quantities in our tables and figures. The reader may for convenience think of the numbers quoted as being in degrees. When the model potential with repulsive tails is used one has the additional parameter α. We have not exhaustively explored this three-dimensional parameter space. We have concentrated primarily in regions where the ratios T_c/ω_0 and ω_0/ε_F are relatively large, and the coherence length is small. The acceptable values of α are restricted by the condition that $D(0)<0$, which is required so that the particle-particle correlation function exists. This gives rise to an upper bound on α.

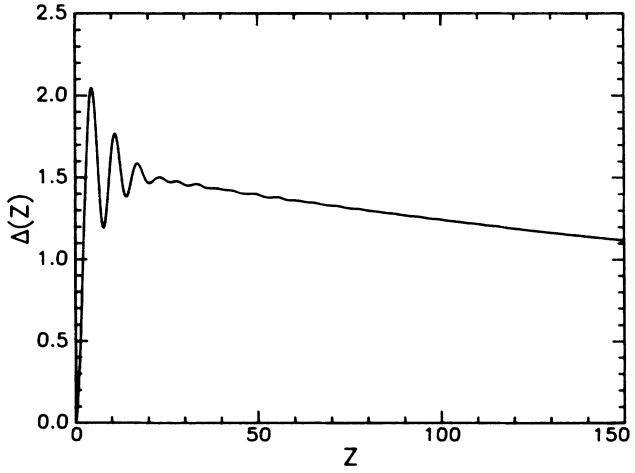

FIG. 8. Gap parameter $\Delta(Z)$ at the surface transition temperature, for $\varepsilon_F=1000$, $\omega_0=300$, $T=50$, and $\alpha=0.8$. $\Delta(Z)$ is defined here up to an overall multiplicative constant (see Sec. III B). Due to the presence of the surface there are strong oscillations and an enhancement of the gap close to the surface. In this case $\Delta(Z)$ decreases at large Z, reflecting that the bulk is normal.

For the standard attractive potential ($\alpha=0$), we never find any enhancement of the surface transition temperature, although Δ is enhanced near the surface. In particular all the values of $(\varepsilon_F,\omega_0,T)$ listed in Table II, gave, up to the accuracy of the numerical calculation, $T_{cS}=T_{cB}$. All other physically acceptable (i.e., $\varepsilon_F>\omega_0>T$) values of the parameters tried, with ε_F ranging from 10000 to 1000 and T from 5 to 100, have also elicited no difference between T_{cS} and T_{cB}. The situation is different when the repulsive tails are added: some of the results for the transition temperature $T_{cS}\neq T_{cB}$ in this case are summarized in Table II. Note that the effect is clearly larger when ξ_0 is smaller. Thus, we see that a small enhancement of the surface transition temperature occurs in some cases.

The corresponding eigenvector $\Delta(b)$ is Fourier transformed to obtain $\Delta(Z)$. Equation (3.3) would be the equation for the actual superconducting gap if the dependence in Δ would be incorporated in $\chi^0_{\rm pp}$. However, here, $\chi^0_{\rm pp}$ is computed for the normal state, i.e., as if Δ were set equal to zero in $\chi^0_{\rm pp}$. Therefore $\Delta(Z)$ is just the profile of the gap at, and just below, the transition, up to a normalization constant which vanishes at that point. This has to be compared with the so-called "local density of states" of Ref. 20. Typical enhancement values of $\Delta(Z)$ near the surface are about 20%, both with and without repulsive

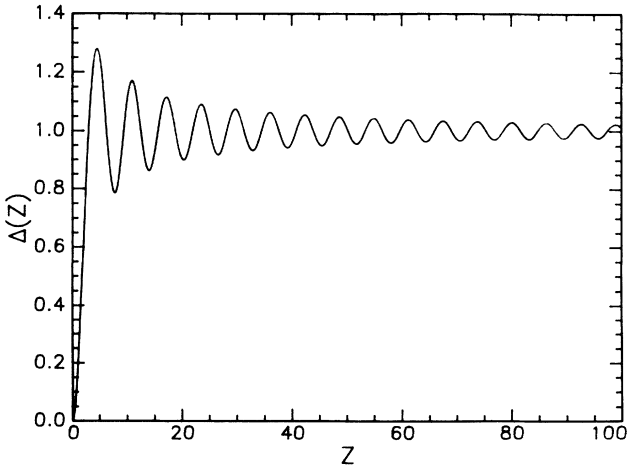

FIG. 9. The gap parameter $\Delta(Z)$ for $\varepsilon_F=10000$, $\omega_0=300$, $T=5$, and $\alpha=0.8$. In that case the bulk is very close to be superconducting and Δ practically tends to a constant at large Z.

tails in the potential. Some of the results are plotted in Figs. 8 and 9.

IV. DISCUSSION

The results of our paper can be summarized as follows.

With the BCS bulk-type attractive square well of Fig. 3(a), an enhancement in Δ is present but there is no surface instability different from the bulk one; the variational method is inconclusive (P_1 is positive) and, to the accuracy of the numerical calculation, no instability is found. If the width ω_0 of such a well becomes infinitely small, then $P_1=0$, one gets the exact analog of the magnetism case, and a surface instability follows. However, this would correspond to an unphysical case, with $\omega_0 \to 0$ (so that $\omega_0 \ll T$) and, consequently, $\bar{V} \to \infty$.

In order to get a surface instability at a temperature where the bulk is still normal it appears to be *necessary* to include repulsive tails such as those of Fig. 3(b) or Fig. 3(c), extending to higher energies than the attractive well, up to roughly ε_F. Such a picture allows b and b' to reach high values and not to be confined to the neighborhood of zero. In other words, this allows for the actual surface effect to play a role by locally enhancing the density of states, yielding the surface instability. However, despite the fact that $T_{cS} > T_{cB}$, the relative increase $\delta T_c / T_c$ is extremely small, typically of order 10^{-3} in the weak-coupling region ($\bar{V} < 1$). A relative increase of order 10^{-2} could be reached only for $\bar{V} \gg 1$ where the present BCS-like calculation would not make sense. For such strong-coupling values, an extension to the present theory would require the solution of the Eliashberg equations as was done in the bulk;[21] this is beyond the scope of the present paper. We also need to deal with small values of ε_F. It is easy to check, through small T/ε_F and small ω_0/ε_F expansions that all the quantities of interest vary inversely proportional to ε_F. Mathematically, in contrast with the magnetism case, the kinetic energies involved in the denominators of $\chi^0_{\rm pp}$ add, so that ε_F survives while in $\chi^0_{\rm ph}$ the same quantities subtract and ε_F disappears. At present we do not know whether there would be ways of experimentally testing our finding that $T_{cS} > T_{cB}$. We need, at any rate, to have samples in confined geometries so that the surface to volume atomic ratio be non-negligible and thus the surface effects do play an important role. A possible course of action would be to reexamine, in confined geometries, the low carrier density superconductors such as the superconducting degenerate semiconductors studied in Ref. 18. Our treatment does not include the enhancement in the bulk T_c found in Ref. 18 but the *relative* increase in the surface transition temperature should survive a more thorough calculation. It would therefore be worthwhile to reexamine those systems experimentally. However $\delta T_c / T_c$ is also higher when T_{cB} itself is high, which is not the case in the superconducting semiconductors. In contrast, the new superconducting oxides offer a better prospect for success since T_{cB} is large; moreover ε_F is low. The ε_F values are not well known in these compounds; however, they are believed to be from 1 eV down to 200 meV. If, in addition, it could be proved in the future that these compounds are strong-coupling superconductors (which is far from being clear at present), then these systems should definitely be investigated in confined geometries or when multiple boundaries are present. A possible experimental test of a T_{cS} larger than T_{cB} might be given by high resolution photoemission experiments such as that described in Ref. 22. The experiments performed there were made on single crystals of $Bi_2Sr_2CaCu_2O_8$. However, only a few layers close to the surface were examined that way, given the mean free path of the photoelectron at the energy that was used. If, in the future, that energy may be made low enough so that the photoelectron mean free path is sufficiently increased and thus a much larger amount of layers can be reached, possibly reflecting the bulk character, then a comparison between the two sets of data would tell whether the superconducting transition temperature near the surface is the same as in the bulk or not.

The gap enhancement near the surface that we have found is a phenomenon more prominent (a 20% effect) and more widespread in parameter space than any enhancement in T_c. It is therefore likely to be of considerably more experimental significance. It is widely reported that critical currents in oxide superconductors are higher in films than in bulk systems.[23] This may be taken as some indication of a gap enhancement, but certainly not as a conclusive confirmation of our theory since other explanations (including experimental artifacts) are possible. Tunneling measurements do give direct evidence about the surface order parameter but published results are, here too, far from conclusive.

Returning to the theory, the model studied here is of course very rough. In particular we do not take into account band structure, possible singularities in the density of states or the anisotropic quasi-two-dimensional character often encountered in the superconducting oxides. On the other hand, in the analogous magnetic case, a number of improvements were examined in order to see whether or not a more realistic model would make the surface instability to be an artifact of the simple model. An interaction I with a nonzero range was considered[24] and it was shown that there is a critical range beyond which the surface magnetic instability disappears. However, it was later shown[16] that, if one takes into account the variation induced by the presence of the surface on the magnitude of I, then a larger range is needed to suppress the surface instability. The increase in the magnitude of I in Ref. 16 has to be compared with the increase in V in Ref. 6: In both cases, the surface instability is favored. With an I constant throughout the sample, the authors of Ref. 25 studied the case where the single-particle potential $\mathcal{V}(z)$ includes a van der Waals attractive well between the system and the wall in a small region $0 < z < a$ close to the surface. This hypothesis proved to reinforce the magnetic instability. Finally it was shown in Ref. 26 that, when the barrier potential at $z=0$ is finite, instead of infinite, the surface magnetic instability disappears when the height of the barrier vanishes, which is reasonable since, ultimately, there will not any longer be a surface and one would recover the bulk system results. Thus, the instability is known to be a very robust phenomenon in the mag-

netic case and it is reasonable to expect that similar conclusions apply in our superconductivity case. The effect of the surface is to induce Friedel-type oscillations away from it, which are strongest within the first few atomic layers, as reflected in the variation of Δ shown on Fig. 8. Physically these strong oscillations act to increase the local density of states near the surface and their existence explains both the magnetic and the superconducting instabilities. We repeat that such effects will be more important for systems with small coherence lengths comparable to the distance over which the Friedel oscillations are strongest. In the strong-coupling regime not only the whole formalism should be reexamined within the framework of Ref. 21, but also fluctuations effects (paraCooperons) should be considered as possibly enhancing the effect. This would require computing the frequency dependence of χ^0 which is beyond the scope of this paper.

ACKNOWLEDGMENTS

One of us (M.T.B-M.) is grateful to L. P. Gor'kov for a fruitful discussion and for attracting her attention to Ref. 6. She also enjoyed useful comments from G. Deutscher. M.T.B-M. and T.G. acknowledge numerous fruitful discussions with C. Bourbonnais and benefited from his suggestions at an early stage of this calculation. O.T.V. acknowledges partial support from the Université de Paris–Sud, the warm hospitality of the Orsay Solid State group, useful conversations with Allen Goldman, and partial support from the National Science Foundation (NSF) under Grant No. DMR-890894.

APPENDIX A: CALCULATION OF χ^0_{pp}

In the half-space system, the bare particle wave function ψ obeys the Schrödinger equation

$$[-\tfrac{1}{2}\nabla^2+\mathcal{V}(z)]\psi=E\psi \tag{A1}$$

with the potential representing the surface

$$\mathcal{V}(z)=\begin{cases}\infty, & z\le 0\\ 0, & z>0\ .\end{cases} \tag{A2}$$

We use atomic units (a.u.). ψ follows from elementary quantum mechanics as was already done in Ref. 13,

$$\psi\propto e^{i\mathbf{k}_\parallel\rho_\parallel}\psi(z)\ , \tag{A3}$$

$$\psi(z)=\begin{cases}\sin(kz), & z\ge 0\\ 0, & z<0\ ,\end{cases} \tag{A4}$$

$$E=k^2/2+\mathbf{k}_\parallel^2/2\ . \tag{A5}$$

Translational invariance is assumed to be conserved parallel to the surface. $\rho_\parallel$ and $\mathbf{k}_\parallel$ are, respectively, the two-dimensional coordinate and momentum parallel to the surface, while z and k are the ones in the direction perpendicular to the surface. We want to calculate the free particle-particle correlation function between the points $\mathbf{R}$ and $\mathbf{R}'$. With ω_n and $\omega_{\nu-n}$ being the Matsubara frequencies of the two particles, we have

$$\chi^0_{pp}(\mathbf{R},\mathbf{R}';i\omega_n)=T\sum_n G(\mathbf{R},\mathbf{R}';i\omega_n)G(\mathbf{R},\mathbf{R}';i\omega_\nu-i\omega_n)\ , \tag{A6}$$

where the one-particle Green's function $G(\mathbf{R},\mathbf{R}';E)$

$$G(\mathbf{R},\mathbf{R}';E)=\sum_{\mathbf{k}_\parallel} e^{i\mathbf{k}_\parallel(\rho_\parallel-\rho'_\parallel)}\mathcal{G}(\mathbf{k}_\parallel,z,z';E)\ . \tag{A7}$$

Then (A6) reads

$$\chi^0_{pp}(\mathbf{R},\mathbf{R}';i\omega_n)=T\sum_n\sum_{\mathbf{k}_\parallel,\mathbf{k}'_\parallel} e^{i(\mathbf{k}_\parallel+\mathbf{k}'_\parallel)(\rho_\parallel-\rho'_\parallel)}\mathcal{G}(\mathbf{k}_\parallel,z,z';i\omega_n)\mathcal{G}(\mathbf{k}'_\parallel,z,z';i\omega_{\nu-n})\ . \tag{A8}$$

Setting $\mathbf{k}_\parallel+\mathbf{k}'_\parallel=\mathbf{K}_\parallel$, we get

$$\chi^0_{pp}(\mathbf{R},\mathbf{R}';i\omega_\nu)=\sum_{\mathbf{K}_\parallel} e^{i\mathbf{K}_\parallel(\rho_\parallel-\rho'_\parallel)}\chi^0_{pp}(\mathbf{K}_\parallel,z,z';i\omega_\nu)\ , \tag{A9}$$

where we have defined

$$\chi^0_{pp}(\mathbf{K}_\parallel,z,z';i\omega_\nu)=T\sum_n\sum_{\mathbf{k}_\parallel}\mathcal{G}(\mathbf{k}_\parallel,z,z';i\omega_n)\mathcal{G}(\mathbf{K}_\parallel-\mathbf{k}_\parallel,z,z';i\omega_{\nu-n})\ . \tag{A10}$$

We thus have to compute (A10). The $\mathcal{G}$'s are easily computed from the ψ's as was done already in Ref. 15. Replacing the sum $\sum_{\mathbf{k}_\parallel}$ by an integral $\int d^2\mathbf{k}_\parallel/(2\pi^2)$, we obtain χ^0_{pp} analogously to χ^0_{ph} in Ref. 15,

$$\chi^0_{pp}(\mathbf{K}_\parallel,z,z';i\omega_\nu)=\sum_{k,k'\ge 0}\int\frac{d^3\mathbf{k}_\parallel}{(2\pi)^2}\sin(kz)\sin(kz')\sin(k'z)\sin(k'z')\times T\sum_n\left[\frac{1}{\Omega(\mathbf{k}_\parallel,k)-i\omega_n}\,\frac{1}{\Omega(\mathbf{K}_\parallel-\mathbf{k}_\parallel,k')-(i\omega_\nu-i\omega_n)}\right]\ . \tag{A11}$$

The sum over n is, as usual, converted to a contour integral and one obtains

$$\chi^0_{pp}(\mathbf{K}_\parallel,z,z';i\omega_\nu)=-\sum_{k,k'>0}\int\frac{d^2\mathbf{k}_\parallel}{(2\pi)^2}\sin(kz)\sin(kz')\sin(k'z)\sin(k'z')\frac{1-f[\Omega(\mathbf{k}_\parallel,k)]-f[\Omega(\mathbf{K}_\parallel-\mathbf{k}_\parallel,k')]}{\Omega(\mathbf{k}_\parallel,k)+\Omega(\mathbf{K}_\parallel-\mathbf{k}_\parallel,k')-\omega} \tag{A12}$$

with

$$\begin{aligned}&\omega=i\omega_\nu\ ,\\&\Omega(\mathbf{k}_\parallel,k)=\mathbf{k}_\parallel^2/2+k^2/2-\varepsilon_F\ ,\end{aligned} \tag{A13}$$

where ε_F is the Fermi energy $\varepsilon_F=k_F^2/2$ in a.u.. We use then the same one-sided cosine Fourier transform as in Ref. 15,

$$\begin{aligned}\chi^0_{pp}(\mathbf{K}_\parallel,q,q';\omega)&=\int_0^\infty\int_0^\infty\chi^0_{pp}(\mathbf{K}_\parallel,z,z';\omega)\cos(qz)\cos(q'z')dz\,dz'\ ,\\\chi^0_{pp}(\mathbf{K}_\parallel,z,z';\omega)&=\int_0^\infty\int_0^\infty\chi^0_{pp}(\mathbf{K}_\parallel,q,q';\omega)\cos(qz)\cos(q'z')dq\,dq'\ .\end{aligned} \tag{A14}$$

Note that z,z',q,q' cannot be negative. On the other hand, numerical constants appearing in front of the sums or the integrals have been omitted because only normalized quantities will be of interest at the end. When needed we have indicated in the text the appropriate multiplicative constants. We find, using some algebra developed in Ref. 15 and in the simple case of $\omega=0$ of interest for the static instability,

$$\begin{aligned}\chi^0_{pp}(\mathbf{K}_\parallel,q,q',0)=-\int\frac{d^2\mathbf{k}_\parallel}{(2\pi)^2}\Bigg\{\sum_{k=-\infty}^{+\infty}\frac{\delta_{q,q'}}{2}\Bigg[\frac{1-f(\mathbf{K}_\parallel-\mathbf{k}_\parallel,k+q)-f(\mathbf{k}_\parallel,k)}{\Omega(\mathbf{K}_\parallel-\mathbf{k}_\parallel,k+q)+\Omega(\mathbf{k}_\parallel,k)}+\frac{1-f(\mathbf{K}_\parallel-\mathbf{k}_\parallel,k-q)-f(\mathbf{k}_\parallel,k)}{\Omega(\mathbf{K}_\parallel-\mathbf{k}_\parallel,k-q)+\Omega(\mathbf{k}_\parallel,k)}\Bigg]\\-\frac{1-f\left[\mathbf{K}_\parallel-\mathbf{k}_\parallel,\frac{(q-q')}{2}\right]-f\left[\mathbf{k}_\parallel,\frac{(q+q')}{2}\right]}{\Omega\left[\mathbf{K}_\parallel-\mathbf{k}_\parallel,\frac{(q-q')}{2}\right]+\Omega\left[\mathbf{k}_\parallel,\frac{(q+q')}{2}\right]}\\-\frac{1-f\left[\mathbf{K}_\parallel-\mathbf{k}_\parallel,\frac{(q+q')}{2}\right]-f\left[\mathbf{k}_\parallel,\frac{(q-q')}{2}\right]}{\Omega\left[\mathbf{K}_\parallel-\mathbf{k}_\parallel,\frac{(q+q')}{2}\right]+\Omega\left[\mathbf{k}_\parallel,\frac{(q-q')}{2}\right]}\Bigg\}\ .\end{aligned} \tag{A15}$$

APPENDIX B: EVALUATION OF G

We want to calculate G as given by (3.17) which implies to first compute (2.24) with (2.6) for the various cutoff models. We first rewrite (2.24) as follows:

$$-A_{pp}(b,b')=\frac{N(0)}{4}\int_{-\varepsilon_F+\varepsilon_F(b+b')^2}^{+\infty}g(\varepsilon_1)w(\varepsilon_1)d\varepsilon_1+\frac{N(0)}{4}\int_{-\varepsilon_F+\varepsilon_F(b-b')^2}^{+\infty}g(\varepsilon_2)w(\varepsilon_2)d\varepsilon_2 \tag{B1}$$

with

$$g(\varepsilon_{1,2})=\frac{\tanh\left[\frac{\varepsilon_{1,2}}{2T}\right]+\tanh\left[\frac{\varepsilon_{1,2}\mp4\varepsilon_Fbb'}{2T}\right]}{2\varepsilon_{1,2}\mp4\varepsilon_Fbb'}\ . \tag{B2}$$

We first consider model (a) with the w given by (2.22). The calculation of $-A_{pp}(b,b')$ is straightforward. We find for the quantities of interest in (3.18) for P_1

$$\begin{aligned}-A^{(a)}_{pp}(b,0)=\frac{N(0)}{2}\Bigg[&\theta(\varepsilon_F-\varepsilon_Fb^2-\omega_0)\int_{-X_0}^{X_0}\frac{\tanh X}{X}dX\\&+\theta(\omega_0+\varepsilon_F-\varepsilon_Fb^2)\theta(\omega_0-\varepsilon_F+\varepsilon_Fb^2)\int_{-X_F(1-b^2)}^{X_0}\frac{\tanh X}{X}dX\Bigg]\end{aligned} \tag{B3}$$

with

$$X_F=\varepsilon_F/(2T),\quad X_0=\omega_0/(2T),\quad -A_{pp}(0,0)=N(0)\int_0^{X_0}\frac{\tanh X}{X}dX\ . \tag{B4}$$

With (2.5) and integration by parts we get

$$-D_{\rm pp}^{(a)}(0)=\frac{N(0)}{2}\int_0^{X_0}\left[\left[1+\frac{X}{X_F}\right]^{1/2}+\left[1-\frac{X}{X_F}\right]^{1/2}\right]\frac{\tanh X}{X}dX\equiv-\chi_{\rm pp}^{0B}\ . \tag{B5}$$

It is of course not surprising to recover for $D_{\rm pp}^{(a)}(0)$ the usual BCS bulk result $\chi_{\rm pp}^{0B}$. In the bulk, and since $X\le X_0\ll X_F$ one usually drops the X term under the square roots. In other words in

$$\chi_{\rm pp}^{0B}=-\tfrac{1}{2}\int_{-\omega_0}^{\omega_0}N(\varepsilon)\frac{\tanh[\varepsilon/(2T)]}{\varepsilon}d\varepsilon\ , \tag{B6}$$

one usually approximates $N(\varepsilon)$ by $N(0)$ through

$$N(\varepsilon)=\frac{\sqrt{2(\varepsilon+\varepsilon_F)}}{2\pi^2}=N(0)\left[1+\frac{X}{X_F}\right]^{1/2}\simeq N(0) \tag{B7}$$

assuming that $\omega_0\ll\varepsilon_F$.

However, here we cannot use this approximation. If we did use it, then we would find that P_1 vanishes identically and thus G would be negative and the surface instability would be demonstrated. Instead without using (B7) we find

$$P_1^{(a)}=\frac{\displaystyle\int_0^{X_0}\left[\left[1+\frac{X}{X_F}\right]^{1/2}-\left[1-\frac{X}{X_F}\right]^{1/2}\right]\frac{\tanh X}{X}dX}{\displaystyle\int_0^{X_0}\left[\left[1+\frac{X}{X_F}\right]^{1/2}+\left[1-\frac{X}{X_F}\right]^{1/2}\right]\frac{\tanh X}{X}dX}>0\ . \tag{B8}$$

Expanding the square root beyond (B7), we find

$$P_1^{(a)}\simeq\frac{T}{\varepsilon_F}\frac{\ln[\cosh(\omega_0/(2T))]}{\chi_{\rm pp}^{0B}/N(0)}\ , \tag{B9}$$

$$P_1^{(a)}\simeq\frac{N(0)}{\chi_{\rm pp}^{0B(a)}}\left[\frac{\omega_0}{2\varepsilon_F}-\frac{T}{\varepsilon_F}\ln 2\right]\quad\text{for }\omega_0\gg T\ . \tag{B10}$$

P_1, although small, is positive. Since P_2 is also positive, G appears as the difference of two small quantities and its sign is not obvious. We will see that, for model (b), where values of X larger than X_0 contribute, this result is drastically modified.

We now consider models with repulsive tails. The algebra is straightforward and we just give the result. For the case of a potential such as that in (2.23) we find

$$-D^{(b)}(0)=\frac{N(0)}{2}[I_1-\alpha(I_2-I_1)]\ , \tag{B11}$$

$$P_1^{(b)}=\frac{N(0)}{-2D^{(b)}(0)}[J_1-\alpha(J_2-J_1)]\ , \tag{B12}$$

with

$$I_{1,2}=\int_0^{X_0,X_F}\left[\left[1+\frac{X}{X_F}\right]^{1/2}+\left[1-\frac{X}{X_F}\right]^{1/2}\right]\frac{\tanh X}{X}dX\ , \tag{B13}$$

$$J_{1,2}=\int_0^{X_0,X_F}\left[\left[1+\frac{X}{X_F}\right]^{1/2}-\left[1-\frac{X}{X_F}\right]^{1/2}\right]\frac{\tanh X}{X}dX \tag{B14}$$

(obviously $J_2>J_1$ and $I_2>I_1$). The bulk transition temperature T_{cB} for this model will be given, using (2.21) by

$$1=(-v)D^{(b)}(0)\ . \tag{B15}$$

We have to ensure that the bare particle-particle correlation function exists, i.e., that $-D^{(b)}(0)>0$. This means an upper bound for α. On the other hand, if we restrict ourselves to the weak-coupling limit when $vN(0)\le 1$ [as already noted, values of $vN(0)\gg 1$ would be allowed only within the Eliashberg framework[21]]. We therefore get

$$-D^{(b)}(0)>1\ \text{ so that }\ \alpha<\frac{I_1-2}{I_2-I_1}\ . \tag{B16}$$

Obviously $\alpha>0$ for the repulsive part to exist but is also smaller than 1 as clear from Fig. 3(a). Otherwise the central part of V, which in reality results from the difference between the attractive and the repulsive contributions to V in the central region, would be zero, an obviously unphysical result. With $\alpha>0$, I_1 must be larger than 2, which restricts the possible range of values for the parameters $\omega_0, T, \varepsilon_F$.

Assuming (B16) is fulfilled, in order for $P_1^{(b)}$ to be negative we need

$$\alpha > \frac{J_1}{J_2 - J_1} \ . \tag{B17}$$

(B16) and (B17) have to be combined with $0 < \alpha < 1$, and thus for this model we end with

$$\frac{J_1}{J_2 - J_1} < \alpha < \min \left[1, \frac{I_1 - 2}{I_2 - I_1} \right] \ . \tag{B18}$$

If the values of $T, \omega_0, \varepsilon_F$ are such that (B18) is fulfilled then $P_1^{(b)} < 0$ and the surface instability is proved.

Similar results have been obtained for the model in Fig. 3(c).

*Permanent address: Center for the Science and Application of Superconductivity, School of Physics and Astronomy, University of Minnesota, Minneapolis, Minnesota 55455.

[1]P. G. de Gennes, Rev. Mod. Phys. **36**, 225 (1964).

[2]P. G. de Gennes, *Superconductivity of Metals and Alloys* (Benjamin, New York, 1966).

[3]L. P. Gor'kov, Zh. Eksp. Teor. Fiz. **37**, 1407 (1960) [Sov. Phys.—JETP **10**, 998 (1960)].

[4]R. G. Boyd, Phys. Rev. **167**, 407 (1968).

[5]J. M. Blatt and C. J. Thompson, Phys. Rev. Lett. **10**, 332 (1963); D. S. Falk, Phys. Rev. **132**, 1576 (1963).

[6]I. N. Khlyustikov and A. I. Buzdin, Adv. Phys. **36**, 271 (1987), and references therein; in particular Ref. 1 and 11 are, respectively, the experimental and the theoretical original papers.

[7]Superconductivity in these materials was first discovered by J. G. Bednorz and K. A. Müller, Z. Phys. B **64**, 189 (1986).

[8]S. S. P. Parkin *et al.*, Phys. Rev. Lett. **60**, 2539 (1988).

[9]P. W. Anderson, J. Phys. Chem. Solids **11**, 26 (1959).

[10]K. Maki, in *Superconductivity,* edited by R. D. Parks (Dekker, New York, 1969), p. 1041.

[11]M. Tinkham, *Introduction to Superconductivity* (McGraw-Hill, New York, 1957), p. 260.

[12]A. F. Andreev, Pis'ma Zh. Eksp. Teor. Fiz. **46**, 463 (1987) [JETP Lett. **46**, 584 (1989)]; A. A. Abrikosov and A. I. Buzdin, *ibid.* **47**, 201 (1988) [**47**, 247 (1988)].

[13]J. P. Muscat, M. T. Beal-Monod, D. M. Newns, and D. Spanjaard, Phys. Rev. B **11**, 1437 (1975), and some earlier partial results referred to therein; see also a review in M. T. Béal-Monod, J. Phys. (Paris) Colloq. **45**, C5-339 (1984).

[14]J. Labbe and J. Bok, Europhys. Lett. **3**, 1225 (1987).

[15]D. M. Newns, Phys. Rev. B **1**, 3304 (1970).

[16]S. C. Ying, L. M. Kahn, and M. T. Béal-Monod, Solid State Commun. **18**, 359 (1976).

[17]J. Bardeen, L. N. Cooper, and J. R. Schrieffer, Phys. Rev. **106**, 162 (1957); **108**, 1175 (1957).

[18]M. L. Cohen, in *Superconductivity,* edited by R. D. Parks (Dekker, New York, 1969), p. 624.

[19]See, for instance, A. L. Fetter and J. D. Walecka, *Quantum Theory of Many Particle Systems* (McGraw-Hill, New York, 1970), pp. 447 and 581.

[20]C. Caroli, P. G. de Gennes, and J. Matricon, J. Phys. Rad. **23**, 707 (1962).

[21]P. B. Allen and R. C. Dynes, Phys. Rev. B **12**, 905 (1975).

[22]J. M. Imer *et al.*, Phys. Rev. Lett. **62**, 336 (1989).

[23]P. Chaudhari *et al.*, Phys. Rev. Lett. **58**, 2684 (1987); J. D. Hettinger *et al.*, *ibid.* **62**, 2044 (1989).

[24]E. Zaremba and A. Griffin, Solid State Commun. **13**, 1697 (1963); Can. J. Phys. **53**, 891 (1975); J. P. Muscat, J. Phys. F **5**, L119 (1975).

[25]D. Spanjaard, D. L. Mills, and M. T. Béal-Monod, J. Low Temp. Phys. **34**, 307 (1979).

[26]J. P. Muscat, J. Phys. F **6**, L117 (1976); **6**, L251 (1976).